

Local strain modification effects on global properties of AlGaIn/GaN high electron mobility transistors

Nahid Sultan Al-Mamun^a, Maxwell Wetherington^b, Douglas E. Wolfe^c, Aman Haque^{a,*}, Fan Ren^d, Stephen Pearton^e

^a Department of Mechanical Engineering, Penn State University, University Park, PA 16802, USA

^b Materials Characterization Laboratory, Penn State University, University Park, PA 16802, USA

^c Department of Materials Science & Engineering, Penn State University, University Park, PA 16802, USA

^d Department of Chemical Engineering, University of Florida, Gainesville, FL 32611, USA

^e Department of Material Science and Engineering, University of Florida, Gainesville, FL 32611, USA

ARTICLE INFO

Keywords:

High electron mobility transistor

Gallium nitride

Strain localization

Electron mobility

ABSTRACT

Performance and reliability of microelectronic devices are governed by the mechanical strain within the device layers. Typically, this is studied with uniformly distributed strain applied externally or internally. The focus of this study is on AlGaIn/GaN high electron mobility transistors (HEMTs), which is expected to be more sensitive to strain due to its piezo-resistive and piezo-electric nature. Accordingly, we hypothesize that even small but localized strain may have significant impact on the overall behavior of a HEMT. To investigate this hypothesis, we introduce highly localized strain relief by milling a $20 \times 30 \mu\text{m}^2$ micro trench about $70 \mu\text{m}$ deep on the backside of an $800 \times 840 \mu\text{m}^2$ size HEMT die. The resulting local relaxation of in-plane residual strain was mapped using micro-Raman technique. Our results show that a decrease of only 0.02% strain can decrease the overall output saturation current up to $\sim 20\%$. The drop of output current is attributed to reduced two-dimensional electron gas (2DEG) sheet carrier density and electron mobility due to the strain relief in the device layers. However, the mechanistic process of strain relief also causes defect generation at the interfaces, which increases leakage current. Our technique for localized strain re-distribution could be an effective tool to surrogate the influence of inherent localized strain build-up across the channel of electronic devices.

1. Introduction

Gallium nitride based (AlGaIn/GaN) high electron mobility transistors (HEMTs) provide unique combination of transport properties in terms of high carrier density, mobility, and critical electric field leading to simultaneously high voltage, high temperature, and high frequency operation [1]. Their attractive properties are attributed to the formation of two-dimensional electron gas (2DEG) at the heterostructure interface resulting from net spontaneous and piezoelectric polarization in the AlGaIn and GaN layers [2]. Therefore, polarization induced 2DEG transport properties are greatly influenced by the strain that evolves during operation of AlGaIn/GaN HEMT. Residual strain is originated during fabrication processes as a result of mismatch in the lattice constants and thermal expansion coefficients between the epitaxial layers and the substrate material [3–5]. The strain level is also influenced by passivation layer, the Al fraction in the AlGaIn barrier layer, and the

thickness of GaN buffer layer and AlGaIn layer [3]. Several studies in literature have reported the effect of external strain on the 2DEG properties of AlGaIn/GaN heterostructure [6–10]. Kang et al. [6] have reported the effect of external strain on the sheet resistance of 2DEG channel in AlGaIn/GaN HEMT using cantilever geometry. Chang et al. [8] and Liu et al. [9] have studied external strain effect on AlGaIn/GaN HEMTs by using three point and four point bending fixtures, respectively. Change in threshold voltage induced by strain modification in the barrier layer of InAlN/GaN HEMTs has been reported by Choi et al. [11]. Azize and Palacios [12] have demonstrated significant change in 2DEG transport properties of AlGaIn/GaN heterostructure by partially thinning the substrate using chemical dry etching. Local substrate removal effects on the AlGaIn/GaN HEMT performance have been reported in separate studies [13,14]. Several studies have also shown that the strain-sensitive 2DEG in AlGaIn/GaN heterostructures can be used as the sensing mechanism for micro-scale pressure sensors [15,16].

* Corresponding author.

E-mail address: mah37@psu.edu (A. Haque).

<https://doi.org/10.1016/j.mee.2022.111836>

Received 15 June 2022; Accepted 21 June 2022

Available online 28 June 2022

0167-9317/© 2022 Elsevier B.V. All rights reserved.

The motivation for this research comes from the observation that the literature has mostly considered uniform distribution of the mechanical strain. In microelectronic devices, strain field generated due to the materials heterogeneity and device features may be localized. Strain could play dominant role for GaN based devices because the material shows both piezoresistive and piezoelectric behavior. To study localized strain effects, we introduce a micro trench on the backside of an AlGaN/GaN HEMT and study the global transport properties.

2. Materials & methods

Commercially available depletion mode GaN HEMT (CGHV1J006D, Wolfspeed®) on 4H-SiC substrate with rated power, frequency, and breakdown voltage of 6 W, 18GHz, and 40 V, respectively, were used. The epitaxial structure of $6 \times 200 \mu\text{m}$ long HEMT is grown on $100 \mu\text{m}$ of 4H-SiC substrate with a $1.4 \mu\text{m}$ of iron-doped GaN buffer layer, $\sim 20 \text{ nm}$ of $\text{Al}_{0.22}\text{Ga}_{0.78}\text{N}$ barrier layer, $\sim 1 \text{ nm}$ of AlN interlayer between the buffer and barrier layer, and $\sim 50 \text{ nm}$ of AlN nucleation layer between the buffer and substrate [17,18]. The gate length is $0.25 \mu\text{m}$ with gate to drain and gate to source spacings of $\sim 3 \mu\text{m}$ and $\sim 1.5 \mu\text{m}$, respectively. The overall die size is $\sim 800 \times 840 \mu\text{m}^2$. In order to locally modify the strain in the AlGaN/GaN heterostructure, a $70 \mu\text{m}$ deep $20 \times 30 \mu\text{m}^2$ rectangular pattern was cut on the substrate underneath the AlGaN/GaN channel using FEI Helios Nanolab 660 dual beam focused ion beam (FIB) equipped with gallium (Ga) ion source. The FIB milling was carried out at 30 kV of accelerating voltage and 65 mA of current. Electrical characterizations were performed on a cascade probe station equipped with Keithley 4200 system. The strain in the GaN layer was characterized by Micro-Raman spectroscopy using a Horiba LabRAM HR Evolution coupled with $100\times$, $\text{NA} = 0.9$ microscope objective. The high-resolution Raman spectra were obtained using 532 nm (Oxxious LCX - Nd:YAG) green laser with an incident laser power $< 4 \text{ mW}$, a confocal hole/slit set to $50 \mu\text{m}$, an 1800 gr/mm grating and a Si-array back-illuminated deep-depleted detector (Horiba - Synapse). Rapid thermal annealing (RTA) was also performed on the FIB trench cut device using AllWin AGA 610 RTA system at 400°C for 40 s in N_2 ambient. All measurements were performed on at least three devices to preserve the reproducibility and consistency of the obtained results.

3. Results

Fig. 1a shows the top side of a HEMT with location of a micro trench on the back side. Micro-Raman frequency shift of E_2 (high) in this region is also shown. Fig. 1b shows the strain map in the GaN layer of the device for both pristine and micro trench conditions. The biaxial residual stress (σ_{xx}) and in-plane strain (ϵ_{xx}) in the GaN layer were determined using frequency shift of E_2 (high) phonon mode compared to the strain-free phonon frequency as detailed in [3]. The calculated residual stresses in the pristine and micro-trench channels are found to vary from 237.7 ± 9.1 to $271.0 \pm 5.9 \text{ MPa}$ and 134.6 ± 6.4 to $197.3 \pm 16.2 \text{ MPa}$, respectively. The stress values can be converted to strain using the elasticity equation to obtain residual strain values ranging from 0.05 ± 0.002 to $0.058 \pm 0.002\%$ and 0.028 ± 0.001 to $0.041 \pm 0.003\%$, respectively. In-plane strain in the AlGaN layer was estimated for both pristine and substrate micro-trench devices using mathematical model proposed by Zhao et al. [19]. These are found to be 7.12×10^{-3} and 5.86×10^{-3} for the pristine and substrate micro-trenched devices, respectively.

The output characteristics (I_{ds} - V_{ds}) of the pristine and micro-trenched GaN HEMTs are shown in Fig. 2a. The drain-source voltage was swept from 0 to 5 V with a step size of 0.05 V, while the gate bias was varied from 0 to -3 V with increments of -0.5 V . The output current shifts downward in case of the substrate micro-trench GaN HEMT compared to the pristine device for all gate bias conditions. The saturation drain current (I_{ds}) of micro-trench device drops $\sim 5.4\%$ at 0 V gate bias. Up to $\sim 20\%$ drop in I_{ds} occurs at -1.5 V gate bias. This observation is in agreement with the study by Lalinsky et al. on a HEMT-based pressure sensor [14]. The transfer curves (I_{ds} - V_{gs}) of both devices are shown in Fig. 2b with drain-source bias varied from 0 to 3 V. The slope of the transfer curves ($\Delta I_{ds}/\Delta V_{gs}$) of substrate micro-trench device is relatively smaller for all drain bias conditions compared to the pristine counterpart representing lower transconductance of former device. However, the threshold voltage ($V_{th} = -2.9 \text{ V}$) of both devices remains almost same, which is very close to the nominal threshold voltage (-3 V) of the GaN HEMT under test. The gate-source I-V curves (I_{gs} - V_{gs}) of both devices are shown in Supplementary Fig. S1. The gate leakage current of the micro-trench device is found to be slightly higher compared to the pristine device.

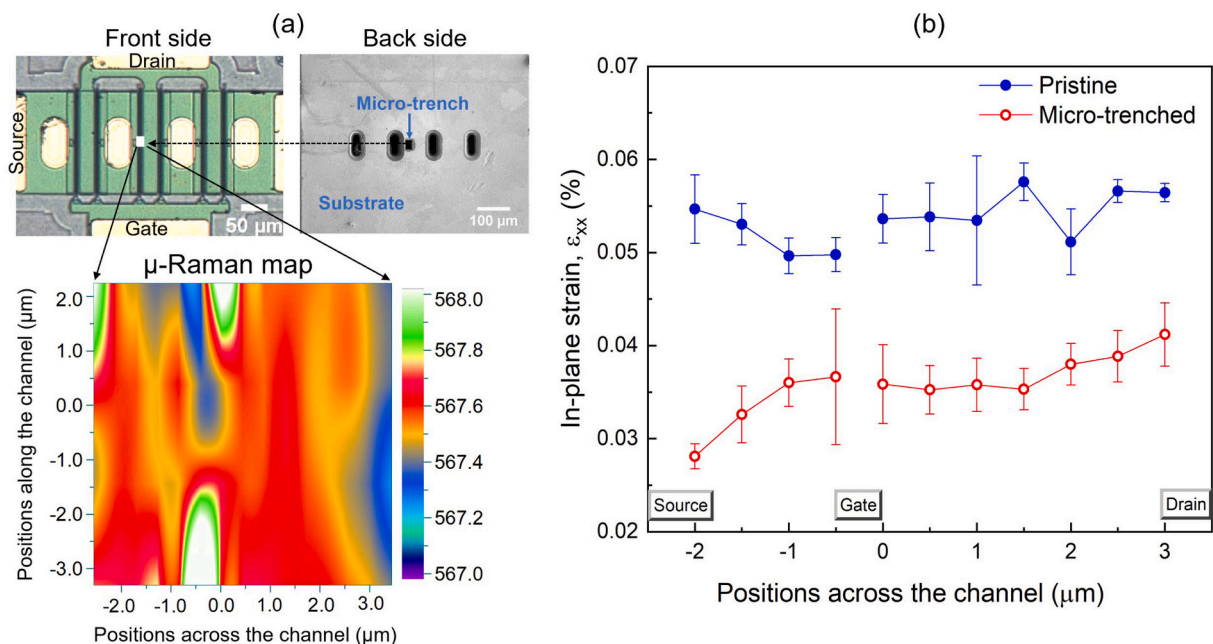


Fig. 1. (a) Micro trench location and μ -Raman E_2 peak shift map (b) in-plane residual strain distribution across the pristine and micro-trenched channels.

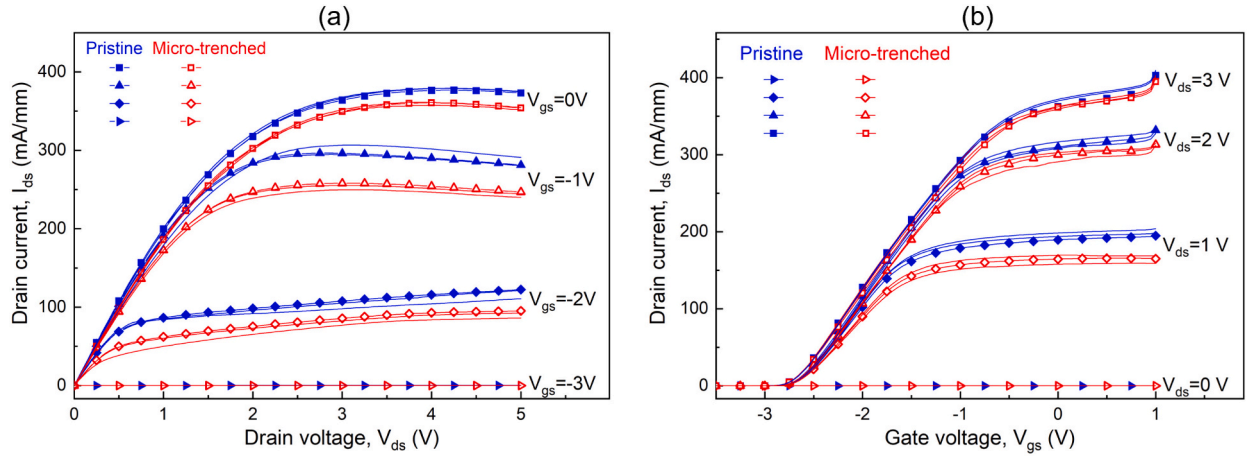


Fig. 2. DC characteristics of pristine and substrate micro-trench devices. (a) Output curves (I_{ds} - V_{ds}) with gate bias from 0 to -3 V and (b) transfer curves (I_{ds} - V_{gs}) with drain bias from 0 to 3 V.

The reduction of output current and slight increase of gate leakage current of the micro-trenched device could possibly originate from three main sources such as defect formation and device degradation, self-heating, and change in device strain level [20]. To study the ion irradiation effect of the FIB, we used the Stopping and Range of Ions in Matter (SRIM) software package [21]. In order to imitate the experimental condition, 30 keV ion energy was used at 0° incident angle during SRIM simulation to find the depth of ion affected zone to be ~ 70 nm. This is shown in Supplementary Fig. S2. This length-scale is too small compared to the remaining substrate thickness under the micro trench ($\sim 30 \mu\text{m}$), suggesting that the substrate micro trench may not influence the device layers. Self-heating effect is not relevant for this study, otherwise the drain saturation current difference between two devices should have increased with the increase of gate bias. But such trait is not observed in the I_{ds} - V_{ds} characteristics, as evident in Fig. 2a. Therefore, we suggest that the localized strain relief due to the micro trench is the dominant factor in the output and transfer characteristics observed in Fig. 2. The localized strain redistribution induced global electrical response of the micro-trench device is independent of location of the trench along the device channel. However, micro-trench far away from the channel does not have any noticeable effect on the electrical properties of the device.

To investigate further, we measured C-V curves of the pristine and micro-trenched devices at a frequency of 1 MHz using the source and

gate contacts for gate bias ranging from -4 V to 0 V with a voltage step of 0.05 V (shown in Supplementary Fig. S3). The 2DEG sheet carrier density (n_{2D}) can be obtained by integrating the C-V curves as described in [22,23]. The calculated n_{2D} of both devices at different gate biases are presented in Fig. 3a. The 2DEG sheet carrier density of the micro-trenched device is found to be slightly lower compared to the pristine device with maximum 2.9% difference at zero bias condition. We also estimated the electron drift mobility (μ_n) of the 2DEG as described in [23,24]. The electron mobility at different gate biases is shown in Fig. 3b. The mobility of the substrate micro-trench device is found to be significantly lower compared to the pristine device at all gate bias conditions. The combined effect of lower 2DEG sheet density and mobility, i.e., lower value of $n_s\mu_n$, represents higher on-resistance of the substrate micro-trench device, which supports the results presented in Fig. 2.

4. Discussion

Since identical devices are used in this study, the observed variation in sheet carrier density and electron mobility between two devices should be related to difference in strain distribution within the devices. The micro-trench is cut right underneath the HEMT channel. Such partial removal of substrate relaxes the pre-existing residual stress in device layers at the vicinity of the micro-trench. This localized stress-relief, in

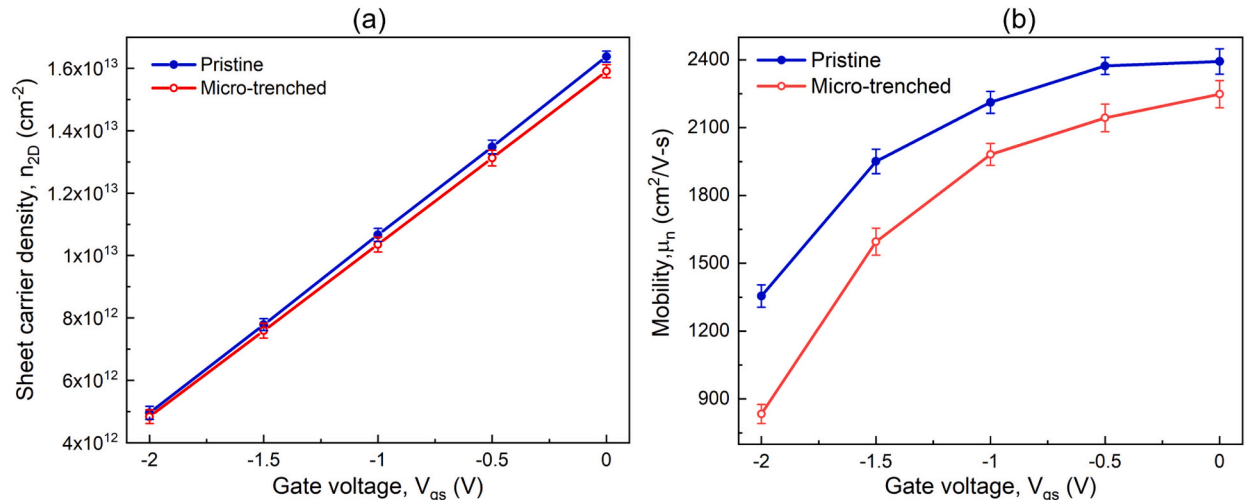


Fig. 3. (a) Sheet carrier density and (b) electron mobility of 2DEG channel of pristine and substrate micro-trench devices at different gate biases.

turn, decreases the magnitude of piezoelectric polarization effect - leading to reduced 2DEG transport properties. The difference in 2DEG electron mobility of two devices can be explained by dominant scattering mechanisms. Since the electron mobility increases with the increase of sheet carrier density at all gate bias condition, LO phonon scattering and interface roughness scattering can be ignored for both devices [24]. Furthermore, micro trench formation by the FIB milling does not alter the impurity level of the GaN/AlGaIn epitaxial layers, which implies that the difference in ionized impurity scattering between two devices can also be ignored. Therefore, the increase of dislocation scattering and/or polarization coulomb field (PCF) scattering phenomena may lead to reduced electron mobility of the substrate micro-trenched device.

We suggest that the primary effect of localized strain relief is the reduction of the carrier density and electron mobility. A secondary effect could be the increase in the density of defects, particularly at the active layer interfaces. The epitaxial layers of GaN HEMT contain a high density of dislocations originating from substrate lattice mismatch [25,26]. The localized strain relief in the epitaxial layers can result increase of these defects. This is evident from the increased gate leakage in the micro-trenched device compared to the pristine. Besides, higher dislocations are more likely to induce higher dislocation scattering events during operation, which can degrade the device performance reducing the 2DEG electron mobility. The micro-trench may also cause the device to experience higher PCF scattering. The faster increase of 2DEG electron mobility with gate bias of the substrate micro-trench device signifies stronger intensity of PCF scattering compared to the pristine device [27]. In other words, higher slope of μ_s - V_G curve of the micro-trench device represents stronger PCF scattering. Since defects can be annihilated (and thus separated from the strain effects on carrier density and mobility) by annealing, we performed rapid thermal annealing (RTA) at 400 °C for 40 s on the micro-trench device. The output characteristics (I_{ds} - V_{ds}) and C-V curves of the substrate micro-trench device before and after RTA are shown in the Supplementary Fig. S4. From the acquired data, we calculated carrier density and electron mobility. These are shown in Supplementary Fig. S5. The observed improvement in the output current and electron mobility after the RTA indicate that in addition to the elastic strain relief effect on the 2DEG, the micro-trench also introduces some defects that are annihilated by RTA.

5. Conclusion

Effect of mechanical strain on the performance and reliability of electronic devices have been studied extensively in the literature, albeit for uniform strain fields. Piezo-electric semiconductors, such as GaN, may exhibit pronounced effects of strain even if it is localized. To study this hypothesis, we performed localized strain modification on AlGaIn/GaN HEMTs by milling micro-trench and measuring the electrical behavior. The local strain variation negatively impacts the DC current output and gate leakage as a result of reduced 2DEG sheet carrier density and electron mobility due to higher scattering events. The results of this work suggest that uneven distribution of strain within the device can impact the device performance. The FIB operated substrate patterning technique can potentially provide flexibility to modify or tailor the strain distribution of the device locally and therefore, control the transport properties of AlGaIn/GaN HEMTs.

Declaration of Competing Interest

The authors declare that they have no known competing financial interests or personal relationships that could have appeared to influence the work reported in this paper.

Acknowledgements

This work was funded by the Defense Threat Reduction Agency

(DTRA) as part of the Interaction of Ionizing Radiation with Matter University Research Alliance (IIRM-URA) under Contract No. HDTRA1-20-2-0002. The content of the information does not necessarily reflect the position or the policy of the federal government, and no official endorsement should be inferred. A.H. also acknowledges support from the U.S. National Science Foundation (ECCS No. 2015795). The work at UF was also supported by NSF DMR via No. 1856662 (James Edgar). All Raman spectroscopy measurements were performed in the Materials Research Institute in the Materials Characterization Laboratory at Penn State University.

Appendix A. Supplementary data

Supplementary data to this article can be found online at <https://doi.org/10.1016/j.mee.2022.111836>.

References

- [1] M. Meneghini, C. De Santi, I. Abid, M. Buffolo, M. Cioni, R.A. Khadar, L. Nela, N. Zagni, A. Chini, F. Medjdoub, G. Meneghesso, G. Verzellesi, E. Zanoni, E. Matioli, GaN-based power devices: physics, reliability, and perspectives, *J. Appl. Phys.* 130 (2021) 181101, <https://doi.org/10.1063/5.0061354>.
- [2] A.D. Koehler, Impact of Mechanical Stress On AlGaIn/GaN HEMT Performance: Channel Resistance and Gate Current, Ph.D. Thesis, University of Florida, 2011, p. 126. Permanent link: <http://ufdc.ufl.edu/UF00043630/00001>.
- [3] S. Choi, E. Heller, D. Dorsey, R. Vetur, S. Graham, Analysis of the residual stress distribution in AlGaIn/GaN high electron mobility transistors, *J. Appl. Phys.* 113 (2013), 093510, <https://doi.org/10.1063/1.4794009>.
- [4] H.J. Park, C. Park, S. Yeo, S.W. Kang, M. Mastro, O. Kryliouk, T.J. Anderson, Epitaxial strain energy measurements of GaN on sapphire by Raman spectroscopy, *Phys. Stat. Sol. (c)* 2 (2005) 2446–2449, <https://doi.org/10.1002/pssc.200461513>.
- [5] T. Beechem, A. Christensen, D.S. Green, S. Graham, Assessment of stress contributions in GaN high electron mobility transistors of differing substrates using Raman spectroscopy, *J. Appl. Phys.* 106 (2009) 114509, <https://doi.org/10.1063/1.3267157>.
- [6] B.S. Kang, S. Kim, J. Kim, F. Ren, K. Baik, S.J. Pearton, B.P. Gila, C.R. Abernathy, C.-C. Pan, G.-T. Chen, J.-I. Chyi, V. Chandrasekaran, M. Sheplak, T. Nishida, S.N. G. Chu, Effect of external strain on the conductivity of AlGaIn/GaN high-electron-mobility transistors, *Appl. Phys. Lett.* 83 (2003) 4845–4847, <https://doi.org/10.1063/1.1631054>.
- [7] H.-L. Kao, H.-C. Chiu, S.-H. Chuang, H.H. Hsu, AlGaIn/GaN high-Electron-mobility transistors on a silicon substrate under uniaxial tensile strain, *ECS J. Solid State Sci. Technol.* 9 (2020), 045017, <https://doi.org/10.1149/2162-8777/ab8786>.
- [8] Chia-Ta Chang, Shih-Kuang Hsiao, E.Y. Chang, Lu Chung-Yu, Jui-Chien Huang, Ching-Ting Lee, Changes of electrical characteristics for AlGaIn/GaN HEMTs Under Uniaxial Tensile Strain, *IEEE Electron Device Lett.* 30 (2009) 213–215, <https://doi.org/10.1109/LED.2009.2012447>.
- [9] K. Liu, H. Zhu, S. Feng, L. Shi, Y. Zhang, C. Guo, The effect of external stress on the electrical characteristics of AlGaIn/GaN HEMTs, *Microelectron. Reliab.* 55 (2015) 886–889, <https://doi.org/10.1016/j.microrel.2015.03.012>.
- [10] S. Choi, E. Heller, D. Dorsey, R. Vetur, S. Graham, The impact of mechanical stress on the degradation of AlGaIn/GaN high electron mobility transistors, *J. Appl. Phys.* 114 (2013) 164501, <https://doi.org/10.1063/1.4826524>.
- [11] S. Choi, H.J. Kim, Z. Lochner, Y. Zhang, Y.-C. Lee, S.-C. Shen, J.-H. Ryou, R. D. Dupuis, Threshold voltage control of InAlN/GaN heterostructure field-effect transistors for depletion- and enhancement-mode operation, *Appl. Phys. Lett.* 96 (2010) 243506, <https://doi.org/10.1063/1.3446891>.
- [12] M. Azize, T. Palacios, Effect of substrate-induced strain in the transport properties of AlGaIn/GaN heterostructures, *J. Appl. Phys.* 108 (2010), 023707, <https://doi.org/10.1063/1.3463150>.
- [13] G. Pavlidis, D. Mele, T. Cheng, F. Medjdoub, S. Graham, The thermal effects of substrate removal on GaN HEMTs using Raman Thermometry, in: 2016 15th IEEE Intersociety Conference on Thermal and Thermomechanical Phenomena in Electronic Systems (ITherm), IEEE, Las Vegas, NV, USA, 2016, pp. 1255–1260, <https://doi.org/10.1109/ITHERM.2016.7517691>.
- [14] T. Lalinský, P. Hudek, G. Vanko, J. Dzuba, V. Kutis, R. Srnák, P. Choleva, M. Vallo, M. Držák, L. Matay, I. Kostić, Micromachined membrane structures for pressure sensors based on AlGaIn/GaN circular HEMT sensing device, *Microelectron. Eng.* 98 (2012) 578–581, <https://doi.org/10.1016/j.mee.2012.06.014>.
- [15] M.J. Edwards, E.D. Le Boulbar, S. Vittoz, G. Vanko, K. Brinkfeldt, L. Rufer, P. Johander, T. Lalinský, C.R. Bowen, D.W.E. Allsopp, Pressure and temperature dependence of GaN/AlGaIn high electron mobility transistor based sensors on a sapphire membrane, *Phys. Status Solidi C* 9 (2012) 960–963, <https://doi.org/10.1002/pssc.201100371>.
- [16] E.D. Le Boulbar, M.J. Edwards, S. Vittoz, G. Vanko, K. Brinkfeldt, L. Rufer, P. Johander, T. Lalinský, C.R. Bowen, D.W.E. Allsopp, Effect of bias conditions on pressure sensors based on AlGaIn/GaN High Electron Mobility Transistor, *Sensors Actuators A Phys.* 194 (2013) 247–251, <https://doi.org/10.1016/j.sna.2013.02.017>.

- [17] R.S. Pengelly, S.M. Wood, J.W. Milligan, S.T. Sheppard, W.L. Pribble, A review of GaN on SiC high Electron-mobility power transistors and MMICs, *IEEE Trans. Microwave Theory Techn.* 60 (2012) 1764–1783, <https://doi.org/10.1109/TMTT.2012.2187535>.
- [18] K.R. Bagnall, E.A. Moore, S.C. Badescu, L. Zhang, E.N. Wang, Simultaneous measurement of temperature, stress, and electric field in GaN HEMTs with micro-Raman spectroscopy, *Rev. Sci. Instrum.* 88 (2017) 113111, <https://doi.org/10.1063/1.5010225>.
- [19] J. Zhao, Z. Lin, C. Luan, Q. Chen, M. Yang, Y. Zhou, Y. Lv, Z. Feng, A method to determine the strain of the AlGa_N barrier layer under the gate in AlGa_N/AlN/GaN heterostructure field-effect transistors, *Superlattice. Microst.* 79 (2015) 21–28, <https://doi.org/10.1016/j.spmi.2014.12.013>.
- [20] S.K. Oh, M.U. Cho, J. Dallas, T. Jang, D.G. Lee, S. Pouladi, J. Chen, W. Wang, S. Shervin, H. Kim, S. Shin, S. Choi, J.S. Kwak, J.-H. Ryou, High-power flexible AlGa_N/Ga_N heterostructure field-effect transistors with suppression of negative differential conductance, *Appl. Phys. Lett.* 111 (2017) 133502, <https://doi.org/10.1063/1.5004799>.
- [21] J.F. Ziegler, J.P. Biersack, The stopping and range of ions in matter, in: D. A. Bromley (Ed.), *Treatise on Heavy-Ion Science: Volume 6: Astrophysics, Chemistry, and Condensed Matter*, Springer US, Boston, MA, 1985, pp. 93–129, https://doi.org/10.1007/978-1-4615-8103-1_3.
- [22] J. Zhao, Z. Lin, T.D. Corrigan, Z. Wang, Z. You, Z. Wang, Electron mobility related to scattering caused by the strain variation of AlGa_N barrier layer in strained AlGa_N/Ga_N heterostructures, *Appl. Phys. Lett.* 91 (2007) 173507, <https://doi.org/10.1063/1.2798500>.
- [23] Y.J. Lv, X.B. Song, Y.G. Wang, Y.L. Fang, Z.H. Feng, Influence of surface passivation on AlN barrier stress and scattering mechanism in ultra-thin AlN/GaN Heterostructure field-effect transistors, *Nanoscale Res. Lett.* 11 (2016) 373, <https://doi.org/10.1186/s11671-016-1591-6>.
- [24] Y. Lv, Z. Lin, Y. Zhang, L. Meng, C. Luan, Z. Cao, H. Chen, Z. Wang, Polarization Coulomb field scattering in AlGa_N/AlN/GaN heterostructure field-effect transistors, *Appl. Phys. Lett.* 98 (2011) 123512, <https://doi.org/10.1063/1.3569138>.
- [25] D. Jena, A.C. Gossard, U.K. Mishra, Dislocation scattering in a two-dimensional electron gas, *Appl. Phys. Lett.* 76 (2000) 1707–1709, <https://doi.org/10.1063/1.126143>.
- [26] R.P. Joshi, V. Sridhara, B. Jogai, P. Shah, R.D. del Rosario, Analysis of dislocation scattering on electron mobility in GaN high electron mobility transistors, *J. Appl. Phys.* 93 (2003) 10046–10052, <https://doi.org/10.1063/1.1577406>.
- [27] J. Zhao, Z. Lin, Q. Chen, M. Yang, P. Cui, Y. Lv, Z. Feng, A study of the impact of gate metals on the performance of AlGa_N/AlN/GaN heterostructure field-effect transistors, *Appl. Phys. Lett.* 107 (2015) 113502, <https://doi.org/10.1063/1.4931122>.